

**A PROJECT REPORT ON**  
**REMOVAL OF EOG ARTIFACTS AND SEPARATION OF DIFFERENT**  
**CEREBRAL ACTIVITY COMPONENTS FROM SINGLE CHANNEL EEG**

**Submitted in partial fulfilment of requirement for the award of the**  
**degree of**

**BACHELOR OF TECHNOLOGY**  
**IN**

**ELECTRONICS & COMMUNICATION ENGINEERING**

**Submitted by**

V. MANASWI	19091A04A1
B. LAKSHMI	20091A0408
K S. SATHEESH	20091A0416
S. SAI HEMANTH	19091A04H0

**Under the Guidance of**

**Mr. S. Khasim Noor Basha, M.Tech, (Ph.D)**

**Assistant Professor in ECE Department**



**DEPARTMENT OF ELECTRONICS & COMMUNICATION ENGINEERING**

**RAJEEV GANDHI MEMORIAL COLLEGE OF**

**ENGINEERING AND TECHNOLOGY**

**(AUTONOMOUS)**

**Affiliated to J.N.T.U.A - Anantapuramu,**

**Approved by A.I.C.T.E - New Delhi,**

**Accredited By N.B.A & NAAC with 'A+' Grade – New Delhi,**

**NANDYAL -518501, Nandyal Dist. A.P.**

**Year: 2019 - 2023**

**RAJEEV GANDHI MEMORIAL COLLEGE OF ENGINEERING  
& TECHNOLOGY  
(AUTONOMOUS)**

Affiliated to J.N.T.U.A - Anantapuramu, Approved by A.I.C.T.E., New Delhi,  
Accredited By N.B.A & NAAC with 'A' Grade - New Delhi,  
NANDYAL -518501, Nandyal Dist. A.P.



**(ESTD-1995)**  
**CERTIFICATE**

This is to certify that V. Manaswi (19091A04A1), B. Lakshmi (20095A0408), K. S. Satheesh (20095A0416), S. Sai Hemanth (19091A0402) of B.Tech ECE final year has carried out the project work on "Removal of EOG artifacts and separation of different cerebral activity from signal channel EEG" under the esteemed guidance of **Mr. S. Khasim Noor Basha, Assistant Professor** of ECE department, for the partial fulfilment of the award of degree of B.Tech in ECE in R.G.M.C.E.T, Nandyal as a bonafide record of work carried by them under our guidance and supervision.

  
**Head of the Department**

Dr. K. Malikarjuna

M. Tech, Ph.D, MISTE, FICTE, MIE

Professor **Dr. V.N.V. SATYA PRAKASH**

Department of ECE B.Tech, M.Tech, Ph.D MISTE, MIETE, MIE  
Professor

Department of E.C.E.

R.G.M College of Engg. & Tech., (Autonomous)  
NANDYAL - 518 501, Kurnool (Dist), A.P.

  
**Project Guide**

Mr.S. Khasim Noor Basha,

M.Tech,(Ph.D)

Assistant Professor

Department of ECE

**Assistant Professor**

Department of ECE

**RGM College of Engg. & Tech. (Autonomous)**

**NANDYAL - 518 501, Kurnool (Dist), A.P.**

**Signature of the External Examiner:**

**Date:**

05/05/2023



## CANDIDATE'S DECLARATION

We here by declare that the work done in this project titled “**Removal of EOG artifacts and separation of different cerebral activity components from single channel EEG**” submitted towards completion of main project in IV Year II Semester of B. Tech (ECE) at the **Rajeev Gandhi Memorial College of Engineering & Technology**, Nandyal. It is an authentic record of our original work done under the guidance of Mr. S. Khasim Noor Basha Assistant Professor, Dept. of ECE, RGM CET, Nandyal. We have not submitted the matter embodied in this project for the award of any other Degree in any other institutions.

By:

**V. Manaswi      19091A04A1**

**B. Lakshmi      20095A0408**

**K S. Satheesh    20095A0416**

**S. Sai Hemanth 19091A04H0**

Place: Nandyal

Date:

## ACKNOWLEDGEMENT

We manifest our heartier thankfulness pertaining to your contentment over our project guide **Mr. S. Khasim Noor Basha sir**, Assistant Professor of Electronics and communication Engineering department, with whose adroit concomitance the excellence has been exemplified in bringing out this project to work with artistry.

We express our gratitude to **Dr. K. Mallikarjuna sir**, Head of the Department of Electronic and communication Engineering department, all teaching and non-teaching staff of the Electronic and communication Engineering department of Rajeev Gandhi memorial College of Engineering and Technology for providing continuous encouragement and cooperation at various steps of our project.

At the outset we thank our honorable **Chairman Dr. M. Santhi Ramudu sir**, And honorable managing director **Mr. M. Sivaram sir** for providing us with exceptional faculty and moral support throughout the course.

Involuntarily, we are perspicuous to divulge our sincere gratefulness to our Principal, **Dr. T. Jaya Chandra Prasad sir**, who has been observed posing valiance in abundance towards our individuality to acknowledge our project work tangentially.

Finally we extend our sincere thanks to all the **Staff Members** of ECEs Department who have co-operated and encouraged us in making our project successful.

Whatever one does, whatever one achieves, the first credit goes to the **Parents** be it not for their love and affection, nothing would have been responsible. We see in every good that happens to us their love and blessings.

By:

<b>V. Manaswi</b>	<b>19091A04A1</b>
<b>B. Lakshmi</b>	<b>20091A0408</b>
<b>K S.Satheesh</b>	<b>20091A0416</b>
<b>S.Sai Hemanth</b>	<b>19091A04H0</b>

## **ABSTRACT**

The electroencephalogram (EEG) signals are usually interfered by many sources of noise like electrooculogram (EOG), which degrades the signals of interest. It causes the poor performance of the Brain-Computer Interface (BCI) systems. In this work, the problem of removal of EOG artifacts and separation of different cerebral activities found in a single-channel contaminated EEG is addressed. For this purpose, a novel model, based on the combined use of Singular Spectrum Analysis (SSA) and Independent Component Analysis (ICA) with a Stationary Wavelet Transform (SWT) is presented. ICA technique is a highly efficient method, which deals with the multichannel EEG signals. But it is difficult to apply the ICA on single channel EEG. Hence, using SSA, the single channel contaminated EEG signals are converted into multivariate information. Then, the multivariate information is fed to ICA, which separates the source signals as different independent components (ICs). Despite the fact that the ICA method performs excellent source separation, still, some required EEG signal content is present in the IC representing itself as an artifact, and thus dropping it would cause loss of EEG signal content. To avoid this problem, SWT is applied on the artifact IC, which performs the thresholding, to separate the actual artifact and preserve the EEG signal content. Matlab simulations have been done on both synthetically generated and real-life EEG signals and the proposed model is compared with the existing works. It is demonstrated that the proposed model has the best artifact separation performance than all the existing techniques, which is shown in terms of the metric, RRMSE (Relative Root Mean Square Error).

## TABLE OF CONTENTS

<b>CONTENT</b>	<b>PAGE NO</b>
<b>Acknowledgement</b>	<b>i</b>
<b>Abstract</b>	<b>ii</b>
<b>List of Figures</b>	<b>iii</b>
<b>List of Tables</b>	<b>iv</b>

### CHAPTER 1

<b>INTRODUCTION</b>	<b>1</b>
1.1 Introduction to EEG	1
1.2 Brain Rhythms	3
1.3 Artifacts	5
1.4 Types of Artifacts	5
1.4.1 EOG Artifact	5
1.4.2 Eye movement Artifact	6
1.4.3 Muscular Artifact	7
1.4.4 Cardiac Artifact	7

### CHAPTER 2

<b>LITERATURE SURVEY</b>	<b>9</b>
--------------------------	----------

### CHAPTER 3

<b>METHODOLOGY</b>	<b>14</b>
3.1 Existing methods	14
3.1.1 EEMD	14
3.1.2 ICA	15
3.1.3 SSA	16
3.1.4 SSA-ICA	18

3.2 Proposed Method	19
3.2.1SSA-ICA-SWT	19
3.2.2 SWT	20

## **CHAPTER 4**

<b>SOFTWARE DESCRIPTION</b>	<b>23</b>
4.1 MATLAB	23
4.1.1 Typical uses of MATLAB	23
4.1.2 Features of MATLAB	24
4.1.3 Basic building blocks of MATLAB	24
4.2 MATLAB Window	25
4.2.1 Command Window	25
4.2.2 Work space Window	25
4.2.3 Current directory Window	25
4.2.4 Command history Window	26
4.2.5Editor Window	26
4.2.6 Graphics Window	26
4.2.7 Online-help Window	26
4.3 MATLAB Files	27
4.3.1 M-files	27
4.3.2 Script files	27
4.3.3 Function files	27
4.3.4 Mat-files	27
4.4 MATLAB System	27
4.4.1Development Environment	28
4.4.2 MATLAB mathematical function	28
4.4.3 MATLAB language	28
4.4.4 GUI Construction	28
4.4.5 MATLAB application program interface	28
4.5 MATLAB working environment	29
4.5.1 MATLAB desktop	29

4.5.2 Using MATLAB editor to create m-files	30
4.5.3 Getting help	31

## **CHAPTER 5**

<b>EXPERIMENTAL RESULTS</b>	<b>32</b>
5.1 Performance Measures	32
5.1.1 SNR	32
5.1.2 RRMSE	32
5.2 Synthetical Data Results	32
5.3 Real Time EEG Data Results	35
5.3.1 Existing methods results	36
5.3.1.1 EEMD	36
5.3.1.2 EEMD-ICA	37
5.3.1.3 SSA	38
5.3.1.4 SSA-ICA	38
5.5.1 Proposed Method	39

## **CHAPTER 6**

<b>CONCLUSION AND FUTURE SCOPE</b>	<b>40</b>
6.1 Conclusion	40
6.2 Future scope	40
<b>REFERENCES</b>	<b>41</b>



## LIST OF FIGURES

FIG. NO	DESCRIPTION	PAGENO
Fig 1.1:	Electrodes placing	2
Fig 1.2.2:	Brain rhythm waveforms	4
Fig 1.4.1:	EOG Artifact	6
Fig 1.4.2:	Eye movement Artifact	6
Fig 1.4.3:	Muscle Artifact	7
Fig 1.4.4:	Cardiac Artifact	8
Fig 3.2.1:	Representation of three-level decomposition by SSA-ICA with wavelet thresholding technique.	20
Fig 3.2.2:	SWT with three level decomposition.	21
Fig 4.5.1:	Representation of MATLAB window	29
Fig 5.2.1:	(A)Real Time EEG signal (b) Generated EOG model artifact(c) EEG model signal and (d) their addition with SNR 0.5 db.	34
Fig 5.2.2	RRMSE and SNR plots for artifact removed EEG signals using (a)EEMD (magenta) (b)EEMD-ICA (blue) (c) SSA (magenta) (d) SSA-ICA (green) (e)proposed SSA-ICA with threshold (red).	34
Fig 5.3.1.1:	Decomposed cerebral activities of EEG by EEMD method (a)81.783 Hz (b) and (c)beta bands (d)11.474 Hz(e)5.127 Hz(f) EOG Artifact.	36
Fig 5.3.1.2:	Decomposed cerebral activities of EEG by EEMD-ICA method (a)and (e)beta bands (b)5.127 Hz (c) EOG Artifact (d) 11.474 Hz (f)81.783Hz	37

Fig 5.3.1.3: Decomposed cerebral activities of EEG by SSA method.  
(a)67.62Hz (b) and (c) beta bands (d) 11.474 Hz (e) 5.127 Hz (f)EOG Artifact. 38

Fig 5.3.1.4: Decomposed cerebral activities of EEG by SSA-ICA method  
(a)5.127Hz (b) EOG Artifact (c)11.474 Hz (d) 67.62 Hz. 38

Fig 5.3.2.1: Decomposed cerebral activities of EEG by proposed SSA-ICA with  
wavelet thresholding method. (a)5.127Hz (b) EOG Artifact (c)11.474 Hz (d)  
and (f) beta bands (e)Electrode pop. 39

## LIST OF TABLES

<b>TABLE NO</b>	<b>DESCRIPTION</b>	<b>PAGE NO</b>
Table 1.2.1:	Brain rhythms of EEG	3
Table 5.2.3:	SNR Vs RRMSE Values	35



---

## **CHAPTER – 1**

### **INTRODUCTION**

#### **1.1 Introduction to EEG**

Electroencephalography (EEG) [1] is a method to record an electrogram of the spontaneous electrical activity of the brain. As the electrical activity monitored by EEG originates in neurons in the underlying brain tissue, the recordings made by the electrodes on the surface of the scalp vary in accordance with their orientation and distance to the source of the activity. EEG can detect abnormal electrical discharges such as sharp waves, spikes or spike and wave complexes that are seen in people with epilepsy, thus it is often used to inform the medical diagnosis. EEG signals associated with the behavior of human activities such as excited, relaxed, drowsy, coma, sleep disorders, depth of anesthesia, encephalopathies, cerebral hypoxia after cardiac arrest and brain death. Brain cells communicate via electrical impulses and are active all the time, even during asleep.

#### ***How it's done?***

Small metal discs called electrodes are placed on the scalp in special positions. These positions are identified by the recordist who measures the head using the International 10/20 system as shown in the Fig 1.1. This relies on taking measurements between certain fixed points on the head. The electrodes are then placed at points that are 10% and 20% of these distances.

Each electrode site is labelled with a letter and a number. The letter refers to the area of brain underlying the electrode.

- F - Frontal lobe
- T - Temporal lobe
- C - Central lobe
- P - Parietal lobe
- O - Occipital lobe
- Even numbers denote the right side of the head

- Odd numbers denote the left side of the head.

An electroencephalogram (EEG) records activity in the brain. Your brain constantly produces tiny electrical signals. During an EEG test, small sensors, called electrodes, are placed on your scalp. The electrodes are connected by wires to an EEG machine. Electrodes are attached using a special paste glue or paste. The electrodes pick up the electrical signals from your brain and record them on a computer. They only pick up the electrical signals. The electrical signals look like wavy lines that show your brainwave patterns. The EEG test can only show your brainwave patterns at the time the test is carried out. At different times, your brainwave patterns may be different. A highly trained specialist, called a clinical neurophysiologist, can recognise if your EEG test shows a brainwave pattern that is different to most other people.

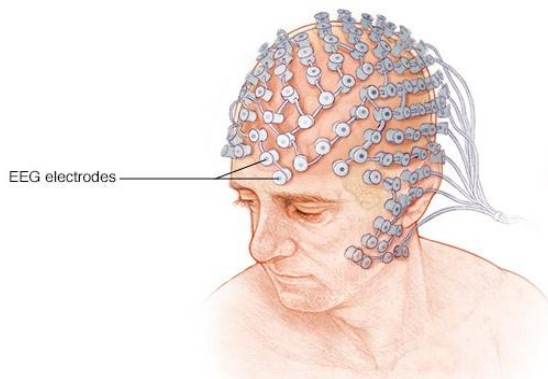


Fig 1.1:Electrodes placing

### ***Why it's done?***

An EEG [2] can find changes in brain activity that might be useful in diagnosing brain disorders, especially epilepsy or another seizure disorder. An EEG might also be helpful for diagnosing or treating:

- Brain tumours
- Brain damage from head injury
- Brain dysfunction that can have a variety of causes (encephalopathy)
- Sleep disorders
- Inflammation of the brain (herpes encephalitis)
- Stroke



An EEG might also be used to confirm brain death in someone in a persistent coma. A continuous EEG is used to help find the right level of anaesthesia for someone in a medically induced coma.

### **1.2 Brain Rhythms**

Many brain disorders are diagnosed by visual inspection of EEG signals. The clinical experts in the field are familiar with manifestation of brain rhythms in the EEG signals[3]. In healthy adults, the amplitudes and frequencies of such signals change from one state of a human to another, such as wakefulness and sleep. The characteristics of the waves also change with age. There are five major brain waves distinguished by their different frequency ranges. These frequency bands from low to high frequencies respectively are called alpha ( $\alpha$ ), theta ( $\theta$ ), beta ( $\beta$ ), delta ( $\delta$ ), and gamma ( $\gamma$ ) as shown in Table 1.2.1.

<b>Serial Number</b>	<b>Brain Rhythm</b>	<b>Frequency Range</b>	<b>State of the brain</b>
1	Delta( $\delta$ )	1-4 Hz	Sleeping / unconscious
2	Theta( $\theta$ )	4-8 Hz	Imagination
3	Alpha( $\alpha$ )	8-13 Hz	Calm consciousness
4	Beta( $\beta$ )	13-30 Hz	Focussed consciousness
5	Gamma( $\gamma$ )	>30 Hz	Peak performance

Table 1.2.1:Brain Rhythms of EEG

Delta and theta rhythms are low-frequency EEG patterns that increase during sleep in the normal adult. Delta waves lie within the range of 0.5–4 Hz. These



waves are primarily associated with deep sleep and may be present in the waking state.

Theta waves lie within the range of 4–7.5 Hz. A theta wave is often accompanied by other frequencies and seems to be related to the level of arousal.

Alpha waves appear in the posterior half of the head and are usually found over the occipital region of the brain. For alpha waves the frequency lies within the range of 8–13 Hz. An alpha wave has a higher amplitude over the occipital areas and has an amplitude of normally less than 50  $\mu\text{V}$ .

A beta wave is the electrical activity of the brain varying within the range of 14–26 Hz. A beta wave is the usual waking rhythm of the brain associated with active thinking, active attention, focus on the outside world, or solving concrete problems, and is found in normal adults.

Gamma The frequencies above 30 Hz (mainly up to 45 Hz) correspond to the gamma range (sometimes called the fast beta wave) are located in the frontal central area[3]. The gamma wave band has also been proved to be a good indication of event-related synchronization (ERS) of the brain as shown in Fig 1.2.2.

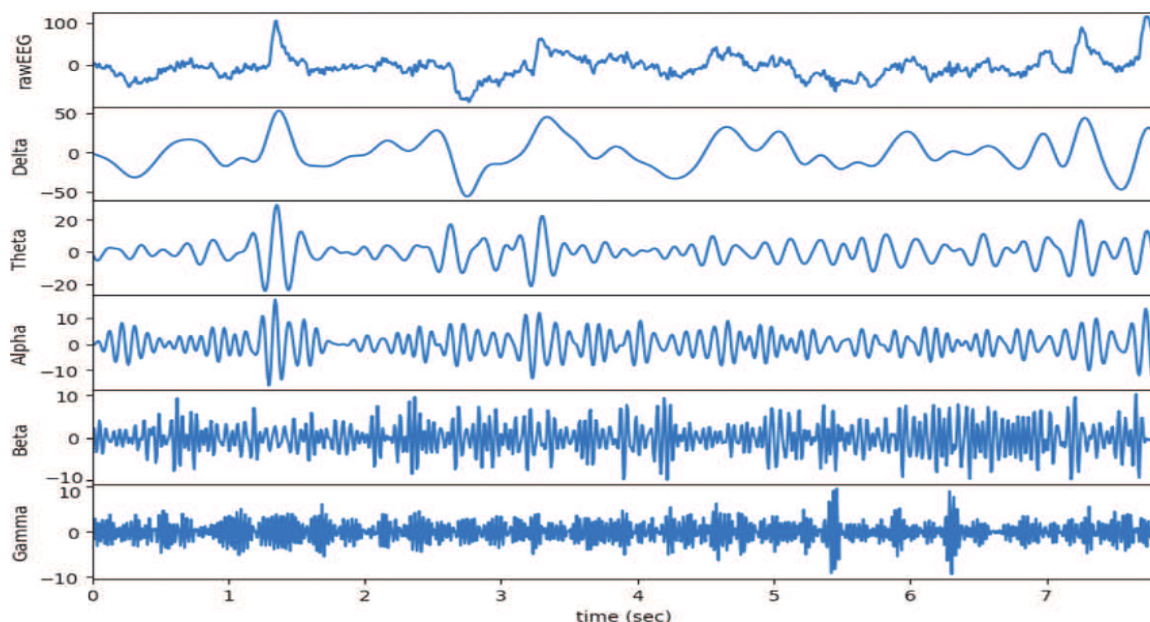


Fig 1.2.2: Brain rhythm waveforms



### **1.3 Artifacts**

Signal artifacts are more significant while collecting EEG data from recording systems [4,5]. These artifacts can contaminate the quality of EEG data. In this regard, a comprehensive knowledge of the types of artifacts is requisite to remove the artifacts or noise efficiently. Artifacts are unwanted signals which are mainly originated from environment noise, experimental error and physiological artifacts. Electroencephalogram signals are the neurophysiologic estimation of the electrical activity of the cerebrum, and these are mostly interfered by unwanted signals or noise called artifacts. Artifacts causes due to eye movement, heartbeat, movement due to the head or electrodes, activity of muscles, breathing, etc. Some artifacts, such as eye links, produce voltage changes of much higher amplitude than the endogenous brain activity. In this situation the data must be discarded unless the artifact can be removed from the data.

### **1.4 Types of Artifacts**

- Eye blink artifact
- Eye movement artifact
- Muscle artifact
- Cardiac artifact

#### **1.4.1 EOG Artifact**

Ocular artifacts generate significant artifacts in the EEG recordings [6]. The origin of ocular artifacts is eye movement and blinks which can propagate over the scalp and be recorded by EEG activity. More specifically, eye movement artifacts produce by changes in orientation of the retina and cornea dipole, and blink artifacts caused by ocular conductance due to the alterations of contact of the cornea with eyelid. In addition, because of volume conduction effect, both ocular artifact and EEG activity propagated to head surface and record by the electrodes. Such ocular signals can be recorded using electrooculogram (EOG) as shown in Fig1.4.1. The amplitude of EOG is generally many times greater than EEG and its frequency are similar with the frequency of EEG signals.





Worthy to note that not only EEG data can be contaminated by the EOG, but in turn, EOG can also be contaminated by EEG. Consequently, a bidirectional interference will introduce removal error when we remove EOG artifacts.



Fig 1.4.1:EOG Artifact

### **1.4.2 Eye movement Artifact**

The eyes are electrically charged structures and their movements generate changing electrical fields[7,8]. The eye is a dipole: the cornea is positive and the retina negative. The dipole is seen only when the eye moves. Both lateral and vertical eye movements can cause characteristic deflections on EEG. Eye movement artifacts are typically seen over the front of the head in the channels closest to the eyes, FP1, FP2, F7 and F8, and are bilateral and Synchronous as shown in Fig 1.4.2. Using additional channels (electrooculogram, EOG) to monitor eye movements can distinguish eye movements from frontal or anterior temporal cerebral potentials. Unusual eye movement artifacts can occur when one eye is missing or injured or the retina is abnormal (loses electrical dipole) or when there is a defect in frontal bones. Common artifacts include those with opening and closing eyes (blink artifact), fluttering of the eyelids (at frequencies from 1 to about 15Hz), vertical and horizontal eye movements (slow lateral eye movements during drowsiness, rapid vertical and lateral eye movements during rapid eye movement sleep, saccadic eye movements during scanning or reading, and nystagmus). During blinks, the eyeball rotates upward (Bell's phenomenon), causing the positive end of the dipole to approach the frontal electrodes.



Fig 1.4.2:Eye movement Artifact



### **1.4.3 Muscular Artifact**

Contamination of EEG data by muscle activity is a well-recognized tough problem as it arises from different type of muscle groups [9,10]. These artifacts can be caused by any muscle proximity to signal recording sites contraction and stretch, the subject talks, sniffs, swallows, etc. In theory, muscle artifacts measured by electromyogram (EMG) have a broad distribution from 0 Hz to >200 Hz. The degree of muscle contraction and stretch will affect the amplitude and waveform of artifacts. It is extremely difficult to obtain the activity from a single channel measurement comparing to EOG and eye-tracking. Therefore, EMG artifacts are particularly challenging to eliminate as shown in Fig 1.4.3. Additionally, EMG contamination and EEG have substantial statistical independence from each other both temporally and spatially. This imply that the Independent Components Analysis might be a suitable method to remove EMG contamination.

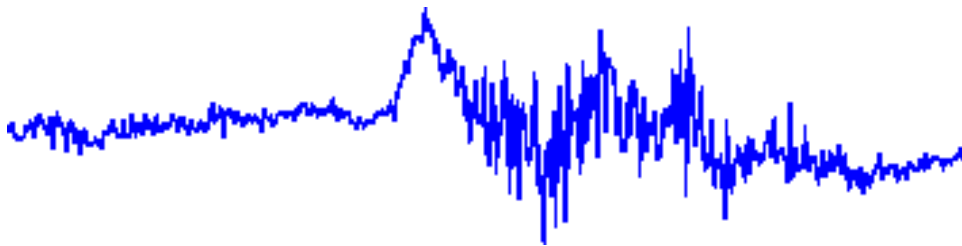


Fig 1.4.3: Muscle Artifacts

### **1.4.4 Cardiac Artifacts**

The heart's electrical activity is another source of spiky potentials [11]. The cardiac QRS complex creates an electrical field that can be detected by EEG, most commonly by referential electrodes placed on the ears. The electrical field of the heart usually extends only to the base of the skull, but may propagate more widely in patients with short thick necks. The electrocardio -graph (ECG) signal is recorded in an additional channel so that cardiac artifacts can be identified by comparing the deflections in the cerebral channels to that in the cardiac channel as shown in Fig 1.4.4. ECG artifact is usually easily identified, but may be more difficult to recognize when the heart rhythm is irregular or



when the QRS has variable morphology. Respiration may cause variability in the electrical axis of the heart, resulting in variable amplitude of the ECG artifact. ECG artifact can be reduced by using bipolar recording montages and by turning the head or extending the neck. When scalp EEG electrodes overlie small arteries, pulse artifact may also be seen as slow waves with a peak 250-300 msec after the peak of the QRS. This can occur in any lead, and may affect several neighbouring electrodes. Ballistocardiograph artifact is a widespread artifact caused by low-amplitude movements of the body during each heartbeat, and is typically only seen when recording at very high sensitivity.



Fig 1.4.4: Cardiac Artifacts



---

## **CHAPTER – 2**

### **LITERATURE SURVEY**

In [12], the authors explained the combination of the empirical mode decomposition (EMD) method and the associated Hilbert spectral analysis has offered a powerful method for nonlinear non stationary data analysis. Central to the present approach is the sifting process to produce the IMFs, which enables complicated data to be reduced into such a form that the instantaneous frequencies can be defined. These IMFs forming the basis of the decomposition are complete and practically orthogonal. The expansion in terms of the IMF basis has the appearance of a generalized Fourier analysis with variable amplitudes and frequencies. It is the first local and adaptive method in frequency– time analysis. A great advantage of EMD and Hilbert spectral analysis is the effective use of the data. In EMD, we have used all the data in defining the longest period component. The foremost advantage of this technique is that, it does not require any prior information of the signal of interest as compared to w-ICA. On the other hand, the major disadvantage of this technique is its sensitivity to noise.

In [13], the authors interpreted the simple wavelet based de-noising technique. Compared with previous methods, this technique neither relies on prior measurements of the EOG, nor makes the distinction between eyeball movement and eye blink artifact correction. Since in real life applications both artifacts are present simultaneously, a method based on such discrimination is then unreliable. Using the time-frequency localization property of the wavelet transform, and the high sampling feature of SWT in all frequency hands, the proposed technique has clearly shown its potential in correcting for low frequency artifacts, such as OAs, while preserving the phase and magnitude of higher frequency components. The disadvantage of a wavelet based de-noising technique for ocular artifact correction of the electroencephalogram is the effective filtering of these ocular artifacts is extremely difficult because their frequency spread (1-50 Hz) overlaps with that of the EEG. Another major



---

drawback of existing frequency based de-noising techniques is that they require continuous recording of electrooculogram (EOG) signals as well.

In [14], the authors evaluated the modified SSA method, called local SSA, to remove, from EEG recordings, high-amplitude and low frequency artefacts which accumulate enough energy to be associated with large eigenvalues of the eigen decomposition. We process the raw data to which no digital filtering has been applied. The method needs the information contained within a single channel only, hence can be applied to each channel separately. Thus, only channels which contain such artefacts need to be processed. Our results confirm that local SSA shows good performance in removing artefacts like eye or head movements, baseline drifts and line noise. In summary, with the method proposed we can separate EEG signal recordings into two components: artefacts and undistorted EEG. It has to be pointed out that local SSA does not require any user intervention to select the components of the reconstruction as in conventional ICA methods these methods are able to separate EOG artifacts only and fail to separate cerebral activity components present within the EEG signals.

In [15], the authors elucidated the EEMD utilizes all the statistical characteristic of the noise: it helps to perturb the signal and enable the EMD algorithm to visit all possible solutions in the finite (not infinitesimal) neighbourhood of the true final answer; it also takes advantage of the zero mean of the noise to cancel out this noise background once it has served its function of providing the uniformly distributed frame of scales, a feat only possible in the time-domain data analysis. In a way, this new approach is essentially a controlled repeated experiment to produce an ensemble mean for a nonstationary data as the final answer. Since the role of the added noise in the EEMD is to facilitate the separation of different scales of the input data without a real contribution to the IMFs of the data, the EEMD is truly a NADA method that is effective in extracting signals from the data. The drawback is that the EEMD-ICA method's efficiency is degraded due to edge effect problem.



In [16], the authors discussed Local mean decomposition (LMD) is a new kind of time–frequency analysis approach which can decompose a signal adaptively into a set of product function (PF) components. In this paper, a modulation feature extraction method-based LMD is proposed. The envelope of a PF is the instantaneous amplitude (IA) and the derivative of the unwrapped phase of a purely flat frequency demodulated (FM) signal is the IF. The computed IF and IA are displayed together in the form of time–frequency representation (TFR). Modulation features can be extracted from the spectrum analysis of the IA and IF. In order to make the IF have physical meaning, the phase-unwrapping algorithm and IF processing method of extrema are presented in detail along with a simulation FM signal example. Besides, the dependence of the LMD method on the signal-to-noise ratio (SNR) is also investigated by analysing synthetic signals which are added with Gaussian noise. In this, each data sequence is named as Product Function (PF). The main advantage of the LMD is, it provides direct accessibility to calculate the instantaneous amplitude and instantaneous frequency from the PF without taking help of intermediate stages. Hence, it overcomes the negative frequency problems. Let these PFs are indicated by  $Y$ . Fast ICA algorithm is applied on  $Y$  as discussed earlier and the PFs generated are added together to produce the required source of the signal. The performance of LMD–ICA depends on the adjustment of parameters in local mean decomposition, which is difficult task to achieve.

In [17], the authors explained DWT and adaptive noise cancellation (ANC) to remove the OAs. The first and most important step of our new method is the construction of a reference signal using DWT. With this reference signal, a new model was established based on ANC; hence, a combination of DWT and ANC is employed. ANC is often used to remove power line interference in EEG signals. However, it does require a reference signal that has proved difficult to obtain in biological systems. In this we apply DWT to the contaminated EEG to derive a reference signal that is used in a further stage of ANC processing. This allows us to lever the biggest advantage of ANC: that it can follow the changes and



---

automatically adjust its parameters to achieve optimal performance of the filter when the statistical properties of the input signal are changing. The effectiveness of this method depends on the quality of DWT derived reference EOG signal, which is decided by proper selection of mother wavelet and the decomposition levels used. Again, the choice of the wavelet and decomposition levels influences the EOG artifact morphology characteristics.

In [18], the authors defined the combined SSA and ANC technique is presented to remove the EOG artifacts from the single channel EEG signals. In this technique, the reference signal (EOG) for ANC is extracted using SSA, thus avoids the use of separate electrodes to record EOG signal. More importantly, unlike DWT-ANC, where the performance is depends on the morphology of the EOG artifact, the proposed SSA-ANC performance is independent of the morphology of the EOG signal, hence better performance is achieved by proposed SSA-ANC. This technique performs better only when, the amplitudes of EEG and EOG signals are high (approximately above 50  $\mu$ v). If these amplitudes are low i.e., approximately below 50  $\mu$ v, its performance is degraded since excess components in the EEG signal frequency band 3–5 Hz are removed [2]. Another drawback in the grouping step is that, the eigen values thresholds are not adjusted automatically and have to be changed manually each time with respect to the window size.

In [19], the authors illustrate the combined SSA-ICA technique to separate/decompose the hidden sources from a single channel EEG signal. Simulation results show that the proposed technique is more efficient to separate the sources when compared with the existing techniques such as w-ICA, EEMDICA, and SSA-ANC. In order to study the effect of window length  $M$  on the performance of SSA-ICA, we have also carried out the simulations for different values of  $M$ , under different noise conditions. Interestingly, the window length of the proposed SSA-ICA technique is independent of signal morphology and noise level. To further validate the performance of the proposed technique, we performed the simulations using two real life single-channel EEG signals. In addition, we have also examined the suitability of the proposed technique for



---

detection of seizures. It is found that the proposed technique showed the superior performance compared with the existing techniques. Moreover, the proposed technique showed a 2.5% improvement in TPR and a 0.02% decrement in FPR compared with the wavelet-based seizure detection method. The disadvantage of this method is that the performance of SSA-ICA method degrades due to the drawbacks of Fast ICA technique, especially some needful EEG signal content present in the IC is misrepresented as artifact, and thus non-inclusion of it, would cause loss of EEG signal content.





---

## CHAPTER – 3

### METHODOLOGY

#### 3.1 Existing methods

##### 3.1.1 EEMD

Ensemble Empirical Mode Decomposition [15] is improve the accuracy of measurements, the ensemble mean is a powerful approach, where data are collected by separate observations, each of which contains different noise. To generalize this ensemble idea, noise is introduced to the single data set,  $x(t)$ , as if separate observations were indeed being made as an analog to a physical experiment that could be repeated many times. The added white noise is treated as the possible random noise that would be encountered in the measurement process. Under such conditions, the  $i^{\text{th}}$  “artificial” observation will be

$$x_i(t) = x(t) + w_i(t). \quad (1)$$

In the case of only one observation, each multiple-observation ensembles is mimicked by adding not arbitrary but different realizations of white noise,  $w_i(t)$ , to that single observation as given in Eq. (1). Although adding noise may result in smaller signal-to-noise ratio, the added white noise will provide a relatively uniform reference scale distribution to facilitate EMD; therefore, the low signal-noise ratio does not affect the decomposition method but actually enhances it to avoid the mode mixing. Based on this argument, an additional step is taken by arguing that adding white noise may help to extract the true signals in the data, a method that is termed EEMD, a truly NADA method.

Before looking at the details of the new EEMD, a review of a few properties of the original EMD is presented:

1. The EMD is an adaptive data analysis method that is based on local characteristics of the data, and hence, it catches nonlinear, nonstationary oscillations more effectively;
2. The EMD is a dyadic filter bank for any white (or fractional Gaussian) noise-only series;



3. When the data is intermittent, the dyadic property is often compromised in the original EMD.

4. Adding noise to the data could provide a uniformly distributed reference scale, which enables EMD to repair the compromised dyadic property; and

5. The corresponding IMFs of different series of noise have no correlation with each other. Therefore, the means of the corresponding IMFs of different white noise series are likely to cancel each other.

With these properties of the EMD in mind, the proposed EEMD is developed as follows:

1. Add a white noise series to the targeted data;
2. Decompose the data with added white noise into IMFs;
3. Repeat step 1 and step 2 again and again, but with different white noise series each time; and
4. Obtain the (ensemble) means of corresponding IMFs of the decompositions as the final result.

### **3.1.2 ICA**

The Independent Component Analysis [20] is a simple but popular model of a signal,  $x \in \mathbb{R}^N$  is to represent it as a linear superposition of vectors  $a_i$ :

$$x = \sum_i s_i a_i \quad (2)$$

where  $s_i$  are the weights or coefficients. This can be written more succinctly in vector-matrix form:

$x = As$ , where  $A = [a_1; \dots; a_N]$  and  $s$  is the vector of coefficients  $s_i$ . Usually, the vectors  $a_i$  are chosen to form a basis in the signal space so that an inverse (analysis) equation is uniquely defined:  $s = Wx$ , where  $W = A^{-1}$ . This has been an extremely popular framework for signal analysis over the years and encompasses the discrete Fourier transform (DFT), the discrete cosine transform (DCT), orthogonal and bi-orthogonal wavelets and the Karhunen-Loeve basis.

If the coefficients  $s_i$  are treated as independent random variables then we have a generative linear statistical model. Furthermore, if we assume that  $A$  is square



and invertible we have the classic ICA model. We can apply such a representation to a scalar time series  $x(t)$  by breaking it up into a sequence of contiguous blocks of length  $N$  and treat these as a sequence of vector observations:

$$x(n) = [x(nN), \dots, x(n(N-1) + 1)]^T \quad (3)$$

where  $n$  is the block index. A standard ICA algorithm then applied to  $x(n)$  can learn a basis that is in some sense 'well matched' to the time series. This is the idea behind learning features using ICA and is closely linked with learning sparse factorial codes.

Since the data in SCICA come from a scalar time series, some thought is required as to how to perform separation. Furthermore, we are often interested in seeing the separated signals back in the original observation domain. In standard ICA, for each source this is achieved through the application of an unmixing and mixing pair of operations:

$$x_s^{(i)} = A_{(:,j)} W_{(i,:)} x \quad (4)$$

where  $x_s^{(i)}$  is the  $i$ th source in the observation domain. One nice property of mapping the sources back to the observation domain is that we have a perfect reconstruction decomposition:

$$x = \sum_i x_s^{(i)} \quad (5)$$

Applying Eq. (3) to the  $n$ th block of the scalar time series, as defined in Eq. (2), gives

$$x_s^{(i)}(nN - k + 1) = A_{(k,i)} \sum_{j=1}^N W_{(i,j)} x(nN - j + 1) \quad (6)$$

where  $j$  and  $k$  index over the  $N$  samples.

### **3.1.3 SSA**

The SSA [18] is a subspace-based technique often used for the analysis of climatic and geophysics time series [21],[22]. Basically, SSA consists of four steps: embedding, decomposition, grouping, diagonal averaging and reconstruction. In the embedding step, firstly the single channel contaminated EEG signal vector  $y$  so obtained is mapped into multivariate data matrix by



arranging J number of lagged vectors of size L, results a trajectory matrix Y of size  $L \times J$ .

$$Y = \begin{bmatrix} y(1) & y(2) & \dots & \dots & y(j) \\ y(2) & y(3) & \dots & \dots & y(j+1) \\ \vdots & \vdots & \dots & \dots & \vdots \\ y(L) & y(L+1) & \dots & \dots & y(N) \end{bmatrix} \quad (7)$$

where  $J = N - L + 1$  and L is the window length and is chosen using the condition i.e.  $L > fs/f$ , where, fs is the sampling frequency and f is frequency of the signal of interest[14],[23]. It is observed that, all the anti-diagonal elements of the trajectory matrix are same, this type of matrix is called hankel matrix. In the second step of SSA, using SVD, the trajectory matrix Y is decomposed into L number of trajectory matrices,  $Y_1, Y_2, \dots, Y_L$ . Let eigenvalues and eigenvectors of a covariance matrix  $C = YY^T$  are denoted as  $\lambda_1, \lambda_2, \dots, \lambda_L$  and  $v_1, v_2, \dots, v_L$ , respectively. Note that the eigenvalues are arranged in the descending order of their magnitudes i.e.,  $\lambda_1 \geq \dots \geq \lambda_L \geq 0$  and also the corresponding eigenvectors  $v_1, v_2, \dots, v_L$ . Then the  $i^{\text{th}}$  trajectory matrix  $Y_i$  is represented as

$$Y_i = \sqrt{\lambda_i} V_i U_i^T \quad i \in \{1, 2, \dots, L\} \quad (8)$$

where,  $u_i = Y^T v_i / \sqrt{\lambda_i}$ , after substitution of  $u_i$ , trajectory matrix  $Y_i$  is represented in terms of eigenvectors of the covariance matrix C and is given by

$$Y_i = v_i v_i^T Y \quad (9)$$

The term  $v_i v_i^T$  represents the subspace corresponding to the  $i^{\text{th}}$  component present in given signal vector y. By projecting the trajectory matrix Y onto that subspace, trajectory matrix for  $i^{\text{th}}$  signal present in y is obtained. Using the trajectory matrices  $Y_i$ 's, the original trajectory matrix Y can be reconstructed using

$$Y = \sum_{i=1}^L Y_i \quad (10)$$

The third and most important step in SSA is grouping the trajectory matrices. The obtained trajectory matrices  $Y_i$  are divided into  $d < L$  groups, based on the magnitudes of the eigenvalues. Let  $K = \{k_1, \dots, k_q\}$  represents the indices



corresponding to the  $q$  eigenvalues of the signal components we are interested in. Then the trajectory matrix for  $K^{\text{th}}$  group can be represented as

$$\hat{Y}_k = \sum_{l=k_1}^{k_q} Y_l. \quad (11)$$

In basic SSA, the indices of eigenvalues  $i = \{1, 2, \dots, L\}$  are grouped into  $d$  disjoint subsets i.e.  $K_1, K_2, \dots, K_d$ , then the trajectory matrix  $Y$  can be represented as

$$Y = \sum_{m=1}^d \hat{Y}_{km} \quad (12)$$

In the final step of SSA, the estimated trajectory matrix of the signal of interest i.e.  $\hat{Y}^I$ , where,  $I$  represents the indices of the eigenvalues of interested signal component, is mapped into single channel signal. For example, let  $y_{kj}$  is an element of  $k^{\text{th}}$  row and  $j^{\text{th}}$  column of the trajectory matrix  $\hat{Y}^I$ , then the  $n^{\text{th}}$  sample of the signal of interest is obtained by averaging anti-diagonal elements of  $\hat{Y}^I$  over all  $k$  and  $j$ , results a single channel signal.

### **3.1.4 SSA-ICA**

In SSA-ICA [19], the SSA is repeatedly used to decompose a single channel EEG to multidimensional information, which is indicated by  $Y$ . In each stage, the EEG is split to lower, higher frequency bands. The division of input signal at every decomposition stage is achieved by the threshold variation to half, i.e.  $fs/4$  at the first decomposition stage,  $fs/8$  at the second decomposition stage and  $fs/16$  at the third decomposition stage etc. and this threshold is generalized as at  $k^{\text{th}}$  stage  $fs/2^{k+1}$ , where  $fs$  is the sampling frequency of input signal and  $k = 1, 2, \dots, k - 1$ . Fast ICA algorithm is applied on  $Y$  as discussed earlier, and decomposed components generated are added together to produce the required source of the signal. The disadvantage of this method is that the performance of SSA-ICA method degrades due to the drawbacks of Fast ICA technique, especially some needful EEG signal content present in the IC is misrepresented as artifact, and thus non-inclusion of it, would cause loss of EEG signal content.



---

## **3.2 Proposed Method**

### **3.2.1 SSA-ICA-SWT**

The proposed SSA-ICA with wavelet thresholding model for three-level decomposition as shown in Fig 3.2.1. In this work,  $y(m)$ , the contaminated single channel EEG, is converted into multivariate information matrix  $Y$  by SSA using the procedure proposed. Fast ICA technique is next applied on the multivariate information matrix  $Y$ , which produces mixing and un-mixing matrices  $A$  and  $W$  respectively, and a matrix of ICs,  $X = WY$  as an output. This is then followed by wavelet thresholding with SWT to eliminate the EOG artifacts and separate the different cerebral activity components present in the single channel contaminated EEG signal. The steps for removing the EOG artifacts from the artifact IC are as follows:

1. Computing the coefficients of the SWT of artifact IC.
2. Compare each and every SWT coefficient with the soft-threshold proposed in [26,27].
3. Set those coefficients greater than the threshold as zero.
4. Perform the inverse SWT to get the reconstructed signal. In this work, it is assumed that large coefficients belong to EOG artifact while the remaining coefficients belong to the wanted signal. The mother wavelet function used was Daubechies db6 [4,5,8,25] and number of decompositions was assumed to be 5.

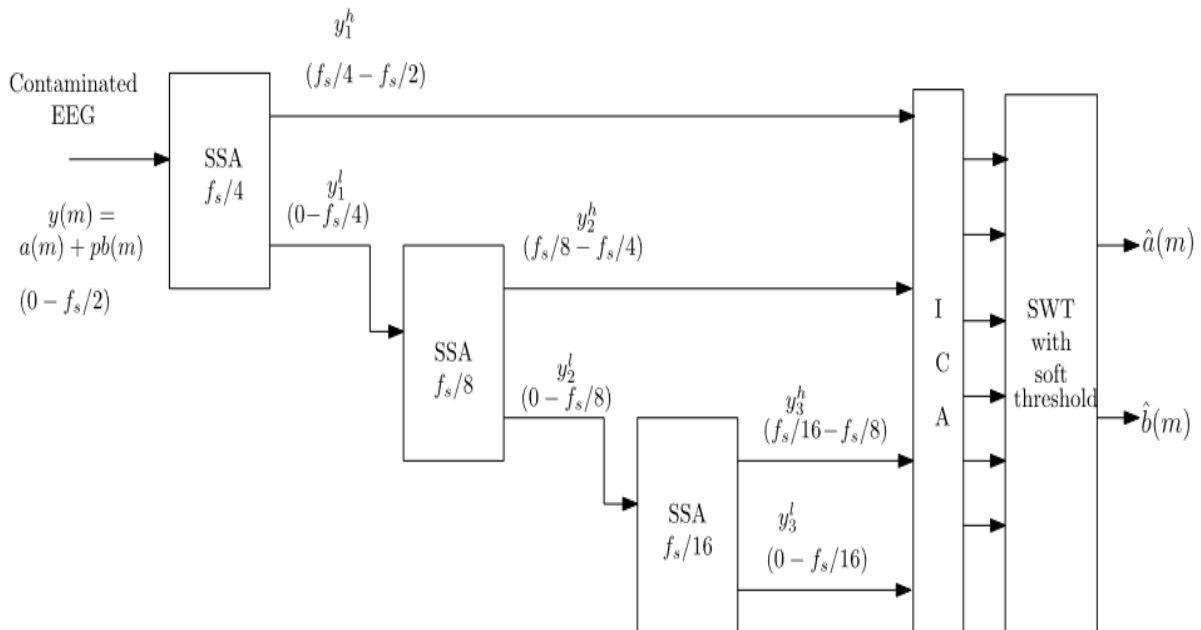


Fig 3.2.1: Representation of three-level decomposition by SSA-ICA with wavelet thresholding technique.

### 3.2.2 SWT

The SWT [23] is also known by a variety of names in the literature including the dyadic wavelet transform (i.e., dyadic in scales), maximal overlap transform and the redundant wavelet transform. SWT is an offshoot of DWT whereby the scales are dyadic but the time steps are not subsampled at each level and hence are not dyadic. In terms of redundancy, the SWT is an intermediate representation of the high redundancy CWT and the nonredundant DWT. It maintains a dyadic sampling of the scales, and therefore maintains a non-redundancy frequency, but carries an almost continuous and uniform sampling time [24]. It has an interest in our study because; unlike the DWT, the redundant representation of SWT makes it shift-invariant and suitable for applications such as edge detection, denoising and data fusion. Since the decimation of its coefficients at each level of the transformation algorithm is omitted, more samples in the coefficient sequences are available, with equal length wavelet coefficients at each level, and hence a better detection can be performed. The DWT cannot provide this feature. Which is critical for a robust detection of the QRS complexes. The SWT has a similar tree structured



implementation as DWT [25], without any decimation (sub-sampling) step. We can write a general transformation equation of SWT based on the coefficients  $c_{j,k}$  calculated as follows:

$$C_{j,k} = \sum_{n \in Z} x(n) \Psi'_{j,k}(n), \quad (13)$$

where  $\Psi'_{j,k}(l)$  is the discrete wavelet defined by:

$$\Psi'_{j,k}(l) = 2^{-j/2} \Psi_{0,0}(2^{-j}(l-k)), \quad (14)$$

The wavelet coefficients are given by  $ca_{j,k}$  and  $cd_{j,k}$ , which represent the approximate (scaling) coefficients and detail (wavelet) coefficients respectively, generated through the convolution chain of the original signal sequence  $x(n)$  and level-adaptive size-varying highpass filter  $H^1$  and lowpass filter  $G^1$  respectively, as shown in Fig. 3.2.1.

Thus, the first scale and detail coefficients  $ca_{1,k}$  and  $cd_{1,k}$  of the SWT can be calculated from a convolution of the input

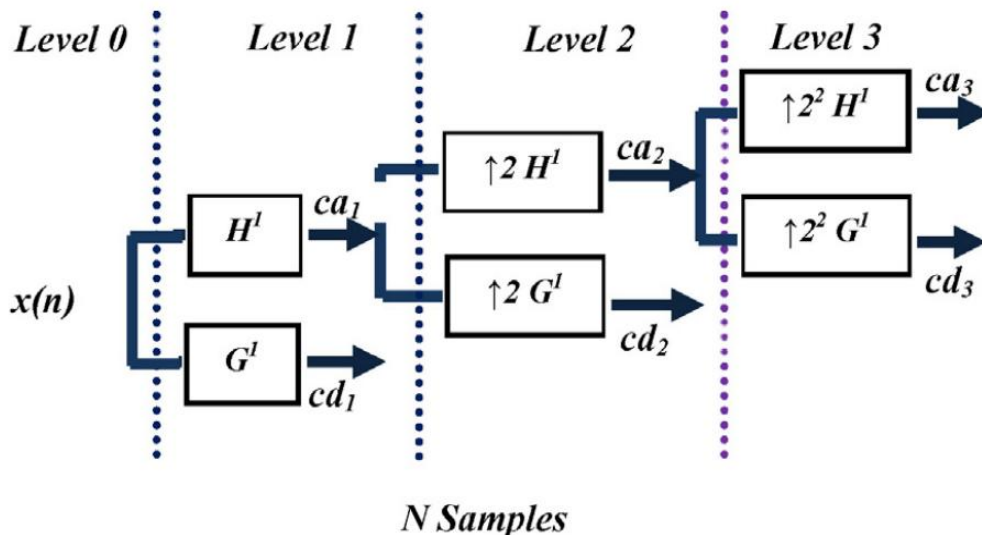


Fig 3.2.2: SWT with three level decomposition.

signal  $x(n)$  with highpass filter  $H^1$  and lowpass filter  $G^1$  respectively, as:

$$\begin{aligned} ca_{1,k}(n) &= H^1(n-r)x(r), \\ cd_{1,k}(n) &= G^1(n-r)x(r). \end{aligned} \quad (15)$$

This can be generalized to the different coefficient's scales by:

$$\begin{aligned} ca_{j,k}(n) &= [\uparrow 2^{j-1} [H_1] * ca_{j-1,k}] = \sum H^j(n-r)ca_{j-1,k}(r), \\ cd_{j,k}(n) &= [\uparrow 2^{j-1} [G_1] * cd_{j-1,k}] = \sum G^j(n-r)cd_{j-1,k}(r). \end{aligned} \quad (16)$$





where  $\uparrow 2^{j-1} [H_1] = H^j(n)$  is the over-sampling of the low-pass filter  $H^{j-1}(n)$  coefficients and  $\uparrow 2^{j-1} [G_1] = G^j(n)$  is the oversampling of the high-pass filter  $G^{j-1}(n)$  coefficients, which are given by:

$$G^i(2n) = G^{i-1}(n)$$

$$G^i(2n + 1) = 0$$

$$H^i(2n) = H^{i-1}(n)$$

$$H^i(2n + 1) = 0 \quad (17)$$

One can clearly see from the previous equation, that the high pass filter  $H^1$  and lowpass filter  $G^1$  are up sampled by a factor of two at each stage. Therefore, the decomposition coefficients (approximation and detail) have the same length  $N_c$  as the original signal  $x(n)$ , where  $N_c = 2^j$ , making the output signal more accurate than the one obtained with DWT.



---

## **CHAPTER - 4**

### **SOFTWARE DESCRIPTION**

#### **4.1 MATLAB**

MATLAB is a high-performance language for technical computing. It integrates computation visualization and programming in an easy-to-use environment. MATLAB stands for matrix laboratory. It was written originally to provide easy access to matrix software developed by LINPACK (linear system package) and EISPACK (Eigen system package) projects. MATLAB is therefore built on a foundation of sophisticated matrix in which the basic element in matrix that does not require pre dimensioning which to solve many technical computing problems especially those with matrix and vector formulations, in a fraction of time.

MATLAB features of applications specific solutions called toolbox. Very important to most users of MATLAB, toolboxes allow learning and applying specialized technology. These are comprehensive collections of MATLAB functions that extend the MATLAB environment to solve particular classes of problems. Areas in which toolboxes are available include signal processing, control system, neural networks, fuzzy logic, wavelets, simulation and many others.

##### **4.1.1 Typical uses of MATLAB**

The typical using areas of MATLAB are

1. Math and computation.
2. Algorithm and development
3. Data acquisition
4. Data analysis, exploration and visualization
5. Scientific and engineering graphics
6. Modelling
7. Simulation
8. Prototyping



9. Application development and including graphical user interface building.

MATLAB is an interactive system whose basic data element is an array that does not require dimensioning. This allow you to solve many technical computing problems, especially those with matrix and vector formulations, in a fraction of the time it would take to write a program in a scalar noninteractive language such as C or FORTRON.

MATLAB features a family of add-on application-specific solutions called toolbox. Very important to most users of MATLAB, toolbox allows you to learn and apply specialized technology. Toolbox is comprehensive collections of MATLAB functions that extend the MATLAB environment to solve particular classes of problems. Areas in which toolboxes are available include signal processing, control systems, neural networks, fuzzy logic, wavelets, simulation and many others.

#### **4.1.2 Features of MATLAB**

1. Advance algorithm for high performancenumericalcomputation, especially in the field matrix algebra.
2. A large collection of predefined mathematical functions and the ability to define one's own functions.
3. Two and three-dimensional graphics for plotting and displaying data.
4. Powerful, matrix or vector oriented high-level programming language for individual applications.
5. Toolboxes available for solving advanced problems in several application areas.

#### **4.1.3 Basic building blocks of MATLAB**

The basic building block of MATLAB is matrix. The fundamental data type is the array. Vectors, scalars, real matrices and complex matrix are handled as specific class of this basic data type. The built-in functions are optimized for vectors operations. No dimension statements are requiring Med for vectors of arrays.



---

## **4.2 MATLAB Window**

The MATLAB works based on five windows

1. Command window
2. Work space window
3. Current directory window
4. Command history window
5. Editor window
6. Graphics window
7. Online-help window

### **4.2.1 Command Window:**

The command window is where the user types MATLAB commands and expressions at the prompt (`>>`) and where the output of those commands is displayed. It is opened when the application program is launched. All commands including user-written programs are typed in this window at MATLAB prompt for execution.

### **4.2.2 Work space Window:**

MATLAB defines the workspace as the set of variables that the user creates in a work session. The workspace browser shows these variables and some information about them. Double clicking on a variable in the work space browser launches the array editor, which can be used to obtain information.

### **4.2.3 Current directory Window:**

The current directory tab shows the contents of the current directory, whose path is shown in the current directory window. For example, in the windows operating system the path might be as follows: `c:\MATLAB\work`, indicating that directory “work” is a sub directory of the main directory “MATLAB”, which is installed in drive c. Clicking on the arrow in the current directory window shows a list of recently used paths. MATLAB uses a search path to find Mfiles and other MATLAB related files. Any file run in MATLAB must reside in the current directory that is on search path.



---

#### **4.2.4 Command history Window:**

The command history window contains a record of the commands a user has entered in the command window, including both current and previous MATLAB sessions. Previously entered MATLAB commands can be selected and re-executed from the command history window by right clicking on a command. This is useful to select various options in addition to executing the commands and is useful feature when experimenting with various commands in work sessions.

#### **4.2.5 Editor Window:**

The MATLAB editor is both a text editor specialized for creating M-files and a graphical MATLAB debugger. The editor can appear in a window by itself, or it can be a sub window in the desktop. In this window one can write, edit, create and save programs in files called M-files.

MATLAB editor window has numerous pull-down menus for tasks such as saving, viewing and debugging files. Because it performs some simple checks and also uses colour to differentiate between various elements of code, this text editor is recommended as the tool of choice for writing and editing M-files.

MATLAB editor window has numerous pull-down menus for tasks such as savings, viewing and debugging files. Because it performs some simple checks and also uses colour to differentiate between various elements of code, this editor is recommended as the tool of choice for writing and editing M-files.

#### **4.2.6 Graphics Window:**

The output of all graphic commands typed in the command window is seen in this window.

#### **4.2.7 Online-help Window:**

MATLAB provides online help for itsbuilt-in functions and programming language constructs. The principal way to get help online is to use the MATLAB help browser, opened as a separate window either by clicking on the question mark symbol on the desktop toolbar, or by typing help browser at the prompt in the command window. The help browser is a web browser integrated into the



---

MATLAB desktop that displays a hypertext markup language document. The help browser consists of two panes, the help navigator plane, used to find information, and the display plane, used to view this information. Self-explanatory tabs other than navigator plane are used to perform a search.

### **4.3 MATLAB Files**

MATLAB has two types of files for storing information. They are

1. M-files
2. MAT – files

#### **4.3.1 M-files:**

These are standard ASCII text file with ‘m’ extension to the file name and creating own matrices using m-files which are text files containing MATLAB code. MATLAB editor or another editor is used to create a file containing the same statements which are typed at the MATLAB command line and save the file under a name that ends in m. There are two types of m-files

#### **4.3.2 Script files:**

M-files with a set of MATLAB commands in it and is executed by typing name of file on the command line. These files work on global variables currently in that environment.

#### **4.3.3 Function files:**

A function file is also an M-file except that the variables in a function file are all local. This type of files begins with a function definition line.

#### **4.3.4 Mat-files:**

These are binary files with. mat extension to that file created by MATLAB when the data is saved. The data written in a special format that only MATLAB can read. These are located into MATLAB with load command.

### **4.4 MATLAB System**

The MATLAB system consists of five main parts:



---

#### ***4.4.1 Development Environment:***

This is the set of tools and facilities that help you see use MATLAB functions and files. Many of these tools are graphical user interface.

It includes the MATLAB desktop and command window, a command history, an editor and debugger, and browser for viewing help, the work space, files and search path.

#### ***4.4.2 MATLAB mathematical function:***

This is a vast collection of computational algorithms ranging from elementary functions like sum, sine, cosine and complex arithmetic to more many functions like matrix inverse, matrix Eigen values, Bessel functions and fast Fourier transforms.

#### ***4.4.3 MATLAB language:***

This is a high-level matrix or array language with control flow statements, functions, data structures, input or output and object oriented programming features. It allows both programming in the small to rapidly create quick and dirty throw-away programs, and programming in the large to create complete large and complex application programs.

#### ***4.4.4 GUI Construction:***

MATLAB has extensive facilities for displaying vectors and matrices as graphs, as well as annotating and printing these graphs. It includes high-level functions for two-dimensional and three-dimensional data visualization, image processing, and animation and presentation graphics. It also includes low-level functions that allow you to fully customize the appearance of graphics as well as to build complete graphical user interface on your MATLAB applications.

#### ***4.4.5 MATLAB application program interface:***

It is a library that allows you to write C and FORTRAN programs that interact with MATLAB. It includes facilities for calling routines from MATLAB, calling MATLAB as a computational engine and for reading and writing MAT-files.



## 4.5 MATLAB working environment

### 4.5.1 MATLAB desktop

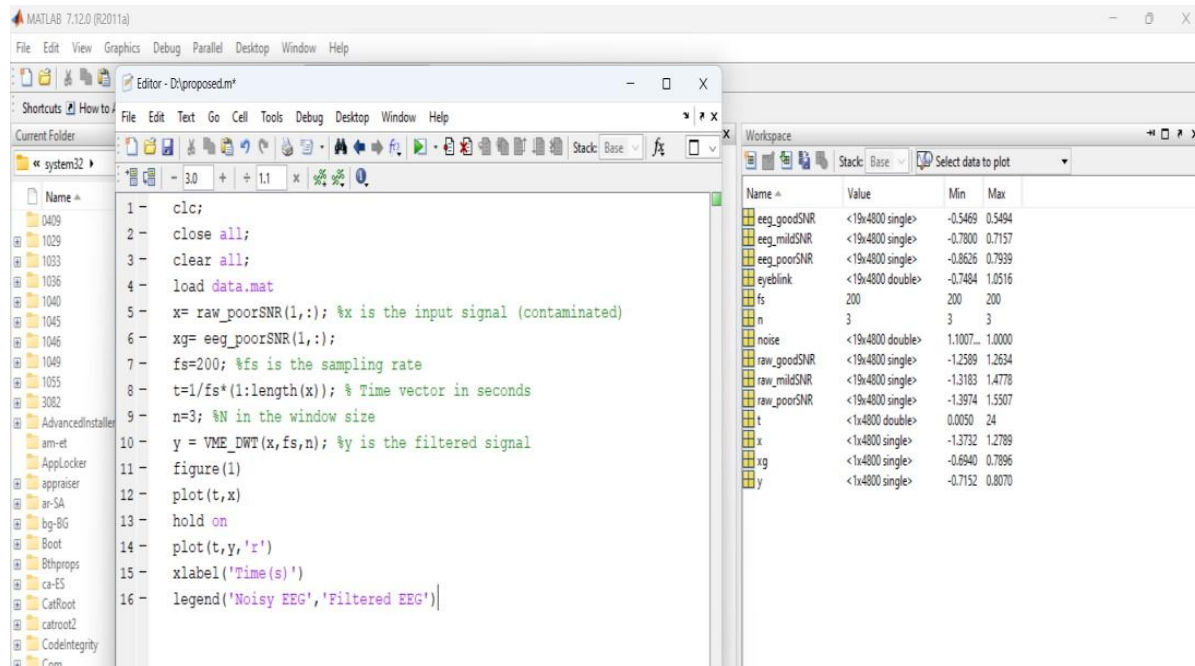


Fig 4.5.1: Representation of MATLAB window

MATLAB desktop is the main MATLAB application window as shown in above fig 4.5.1. The desktop contains five sub windows, the command window, workspace browser, current directory window, command history window, and one or more figure windows which are shown only when the user displays a graphic.

The command window is where the user types MATLAB commands and expressions at the prompt (>>) and where the output of those commands is displayed. MATLAB defines the workspace as the set of variables that the user creates in a work session. The workspace shows these variables and some information about them. Double clicking on a variable in the workspace browser launches the array editor, which can be used to obtain information and income instances edit certain properties of the variable.

The current directory tab above the workspace tab shows the contents of the current directory whose path is shown in the current directory window. For example, in the windows operating system the path might be as follows





C:\MATLAB\work, indicating that directory work is a subdirectory of the main directory MATLAB which is installed in drive. Clicking on the arrow in the current directory window shows a list of recently used paths. Clicking on the button to the right of the window allows the user to change the current directory.

MATLAB uses a search path to find M-Files and other related files, which are organized in directories in the computer file system. Any file run in MATLAB must reside in the current directory that is on search path. By default, the files supplied with MATLAB and math works toolboxes are included in the search path. The easiest ways to see which directories is soon the search path or add to modify as search path is to select set path from the file menu the desktop and then use the set path dialog box. It is good practice to add any commonly used directories to the search path to avoid repeatedly having the change the current directory.

The command history window contains a record of the commands a user has entered in the command window including both current and previous MATLAB sessions. Previously entered MATLAB commands can be selected and re-executed from the command history window by right clicking on a command or sequence of commands. This action launches a menu from which to select various options in addition to executing the commands. This is useful to select various options in addition to executing the commands. This is a useful feature when experimenting with various commands in a work session.

#### ***4.5.2 Using MATLAB editor to create m-files***

The MATLAB editor is both a text editor specialized for creating mfiles and a graphical MATLAB debugger. The editor can appear in window by itself, or it can be a sub window in the desktop. M-files are denoted by the extension.m.

The MATLAB editor window has numerous pull-down menus for tasks such as savings, viewing and debugging files. Because it performs some simple checks and also uses colour to differentiate various elements of code, this text editor is recommended as the tool of choice for writing and editing m-functions. To open the editor type, edit at the prompt opens the m-file filename.m in an editor



---

window is ready for editing. As noted, that the file must be in the current directory or in a directory in the search path.

#### ***4.5.3 Getting help***

The principal way to get help online is to use the MATLAB help browser, opened as a separate window either by clicking on the questions mark symbol on the desktop toolbar or by typing help browser at the prompt in the command window. The help browser is a web browser integrated into the MATLAB desktop that displays a hypertext markup language document. The help browser consists of two windows, the help navigator window, used to find information and the display window, to view the information. Self-explanatory tabs other than navigator pane are used to perform a search.



## CHAPTER-5

### EXPERIMENTAL RESULTS

#### 5.1 Performance Measures

The signal to noise ratio (SNR), relative root mean square error (RRMSE) and Mean Absolute Error (MAE) are computed between the EEG true and artifact signal and filtered EEG signals.

##### 5.1.1 SNR

Signal to noise ratio measures the similarity between two signals. The SNR [19] is expressed as:

$$SNR = \frac{RMS(S_d)}{RMS(p_a)} \quad (17)$$

where,  $p$  is an propagation constant that will decide the SNR of the measured signal.

##### 5.1.2 RRMSE

Relative Root Mean Square Error measures the difference between two signals. The RRMSE [19] is expressed as:

$$RRMSE = \frac{rms(S_d - \hat{S}_d)}{rms(S_d)} * 100 \quad (18)$$

where  $RMS(S_d)$  is the root mean square of the desired source signal and  $RMS(\hat{S}_d)$  is the root mean square of the estimated desired source signal.

Lower RRMSE values indicate better filtering quality.

#### 5.2 Synthetical Data Results

The construction of synthetic EEG signal comprises of two steps: the first step is the generation of EEG model signal and the second step is EOG artifact generation. As the EEG signal is similar to a noise signal since it is non-stationary, the pink noise was considered as the EEG signal model. Next, the EOG artifact signal is generated as one-second duration of EOG epoch and it is placed at 1s intervals in a zero-magnitude 8s signal. Then, for clear visualization of spikes, the high-frequency elements of the EOG epoch were suppressed using the Matlab command "smooth". The interfered synthetic signal  $y(m)$  is



constructed by the addition of the EEG model signal  $a(m)$  and EOG model artifact  $b(m)$  according to the mixing model represented in Eq. (9). The generated EOG model artifact signal  $b(m)$ , EEG model signal  $a(m)$  and their resultant interfered signal  $y(m)$  are shown in Fig. 5.2.1(a), (b), (c), and (d) respectively.

The existing and proposed SSA-ICA with wavelet thresholding methods are applied on synthetically generated EEG signals by varying different signal to noise ratios (SNRs). In this work, for the synthetically generated EEG experiments, the parameter SNR signifies the propagation constant. A low SNR implies high propagation constant; in this case, EOG artifacts are of higher magnitude and can be easily removed. On the other hand, a high SNR value, indicates low propagation constant and identification of EOG component from contaminated EEG record is not efficiently done by all existing methods, because of their various constraints. The propagation constant was assumed to range from 0.1 to 2 corresponding to SNR 4 dB to 0.4 dB respectively. The Fig. 5.2.2 shows, RRMSE plots for the artifact removed EEG by the EEMD, EEMD-ICA, SSA, SSA-ICA and SSA-ICA with thresholding techniques for various SNRs. From Fig. 5.2.2, it is clearly observed that proposed SSA-ICA with thresholding gives better performance than the existing methods in terms RRMSE for different SNRs.

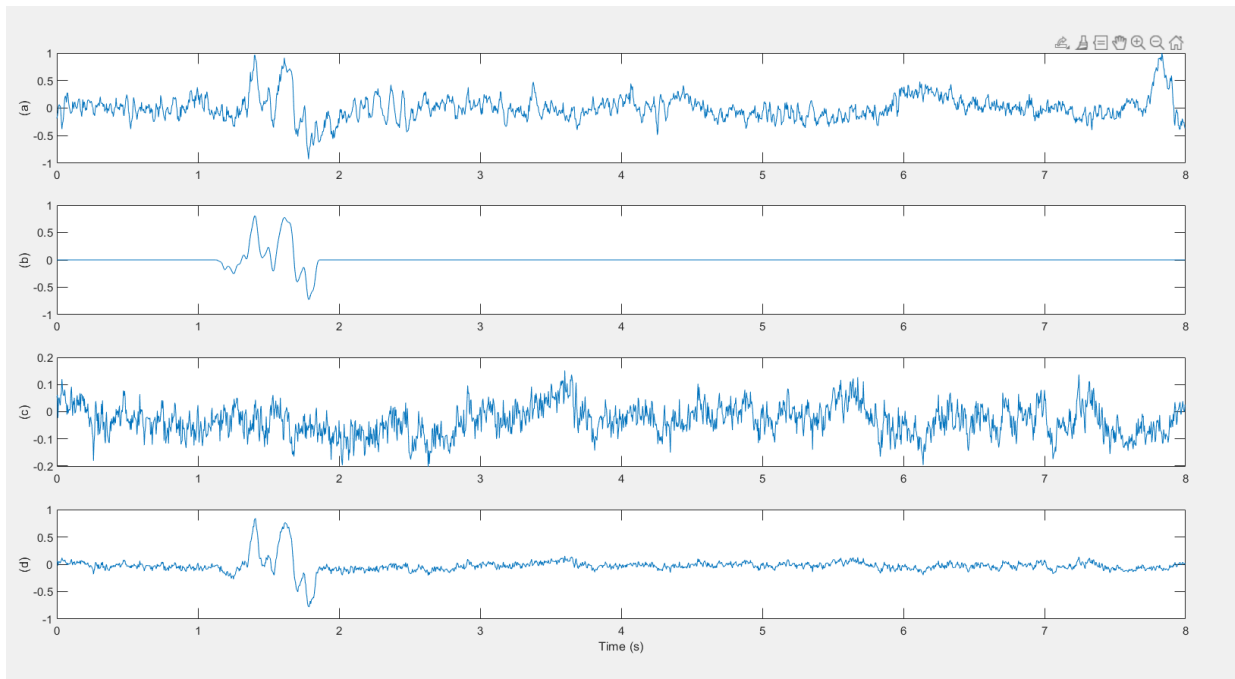


Fig 5.2.1:(a)Real Time EEG Signal (b) Generated EOG model artifact(c) EEG model signal and (d) their addition with SNR 0.5 db.

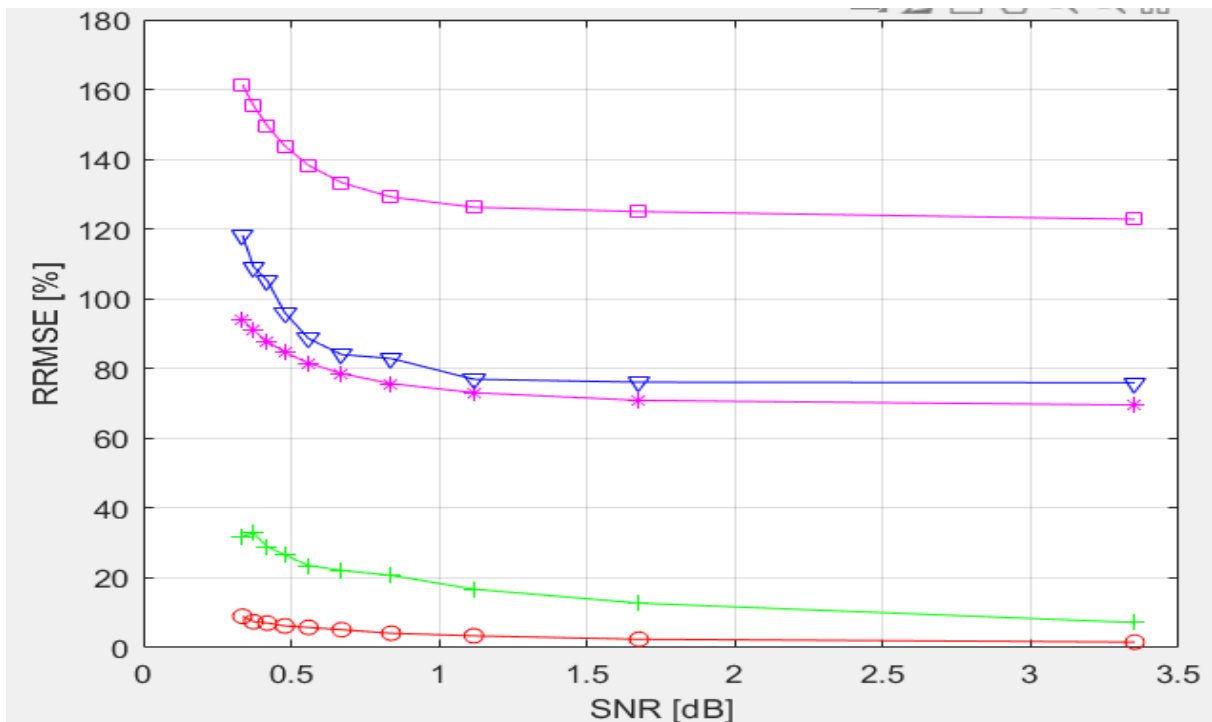


Fig 5.2.2RRMSE and SNR plots for artifact removed EEG signals using (a)EEMD(magenta) (b)EEMD-ICA(blue) (c) SSA(magenta) (d) SSA-ICA(green) (e)proposed SSA-ICA with threshold(red).



SNR	EEMD [15]	EEMD- ICA [15]	SSA [18]	SSA-ICA [19]	SSA-ICA- SWT
0.5	130.741	101.162	84.0405	28.9296	23.3325
1	117.189	86.9122	73.5372	17.948	5.11053
1.5	113.967	76.2692	71.2136	14.8734	3.88844
3	112.548	70.4784	69.7359	7.87243	3.08438

Table 5.2.3:SNR Vs RRMSE Values

### 5.3 Real Time EEG Data Results

The real-time contaminated EEG signals are considered from the EEG information recorded for brain-computer interface motor imagination study [28,29]. This database comprises of 64 records each with 23 channels, which are recorded with 250 Hz sampling frequency. We tested the existing and proposed techniques on several segments (each segment with 2000 samples) and displayed the six segments (each segment 10 trials) of real EEG epochs results. The six segments of mixed EEG epochs with a span of 8 s, which are recorded from the electrode positions. The decomposed levels are assumed as 5 for existing and proposed techniques. This gives five detailed coefficients and one approximate coefficient, i.e., totally six components will be generated. Hence, to map these six components, we assumed the ICA components also as six. This is a limitation of the proposed method. As experimental results on the BCI Competition dataset, with 5 decomposed levels provided best results, hence 5 decomposition levels was used. The separation of EOG artifact and different cerebral activity components present in the mixed EEG signals are shown in Figs. 5.3.1.1(a) – 5.3.2.1(a), for EEMD, EEMD-ICA, SSA, SSA-ICA and proposed SSA-ICA with wavelet thresholding techniques respectively.



### 5.3.1 Existing methods results

The separation of EOG component and other cerebral activity components using EEMD and EEMD-ICA techniques are shown in Fig. 5.3.1.1 and Fig. 5.3.1.2 respectively. Here for efficient separation of sources, we assumed the number of ensembles is 0.2, noise parameter is 50. From Figs. 5.3.1.1 and 5.3.1.2 the separated EOG component is highlighted by the square shape, and, it is observed that, the separation of the EOG component is done poorly.

#### 5.3.1.1 EEMD

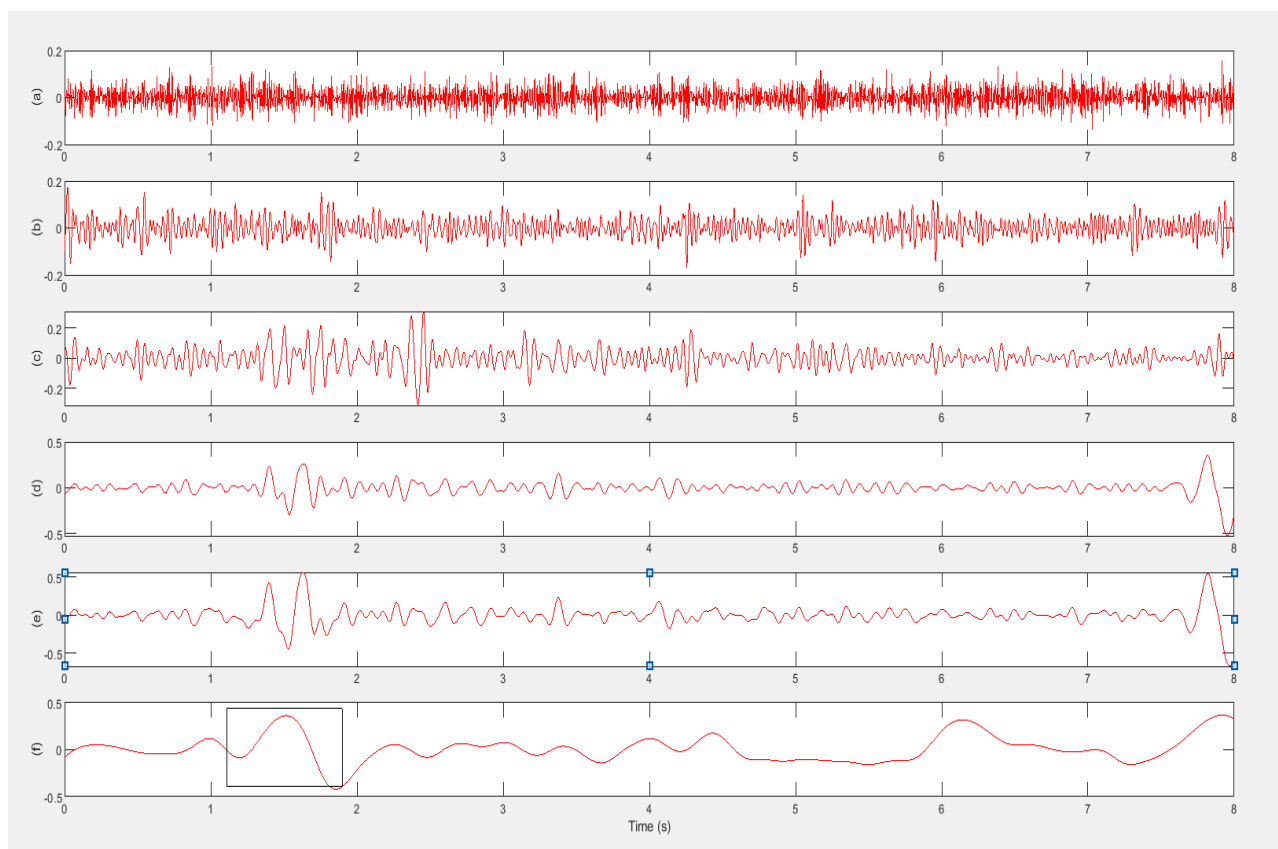


Fig 5.3.1.1: Decomposed cerebral activities of EEG by EEMD method (a) 81.783 Hz (b) and (c) beta bands (d) 11.474 Hz (e) 5.127 Hz (f) EOG Artifact.



### 5.3.1.2 EEMD-ICA

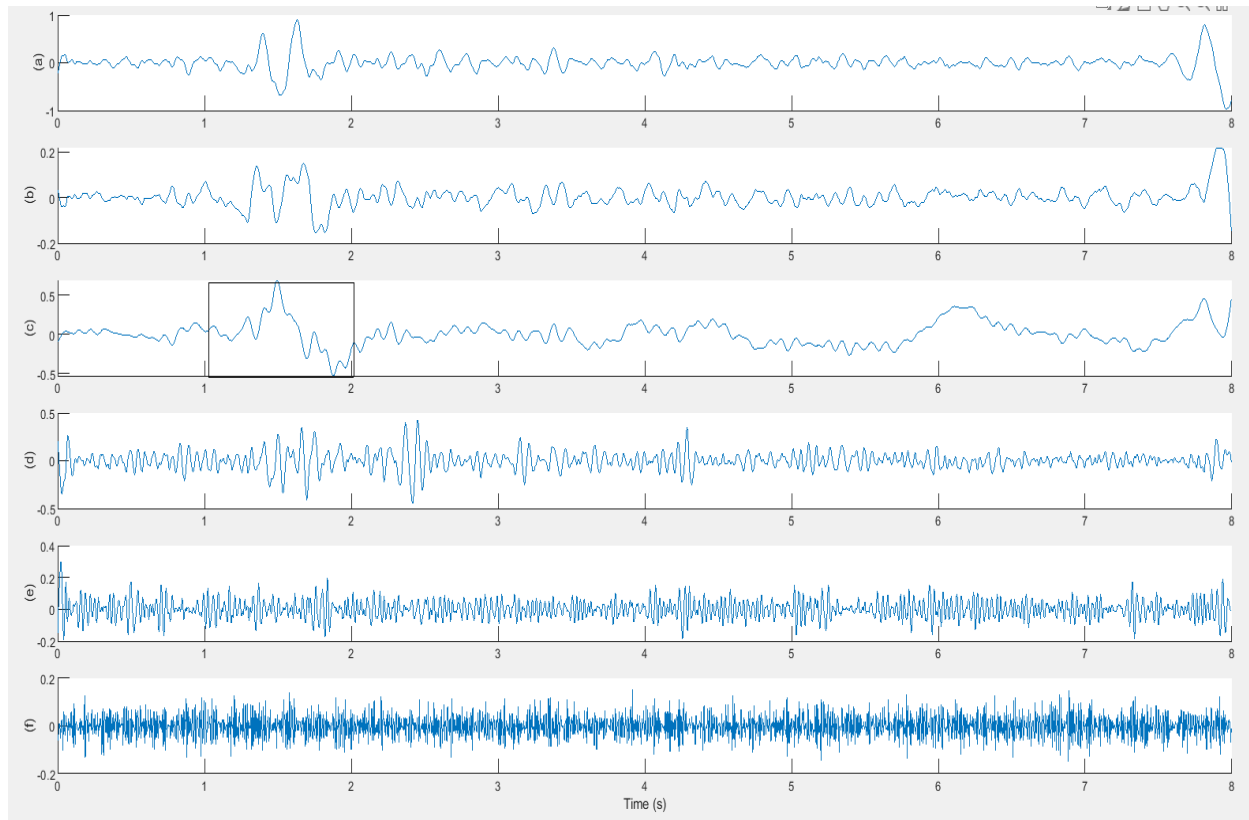


Fig5.3.1.2: Decomposed cerebral activities of EEG by EEMD-ICA method (a) and (e) beta bands (b) 5.127 Hz (c) EOG Artifact (d) 11.474 Hz (f) 81.783 Hz

The separation of EOG component and other cerebral activity components by SSA and SSA-ICA methods are displayed in Fig.5.3.1.3 and Fig.5.3.1.4 respectively. In this, for effective performance the length of SSA window  $L$  is assumed as 50. From Figs.5.3.1.3 and 5.3.1.4 the separated EOG component is highlighted by the square shape, and it can be seen that along with EOG component, some needful EEG information is also separated as artifact.





### 5.3.1.3 SSA

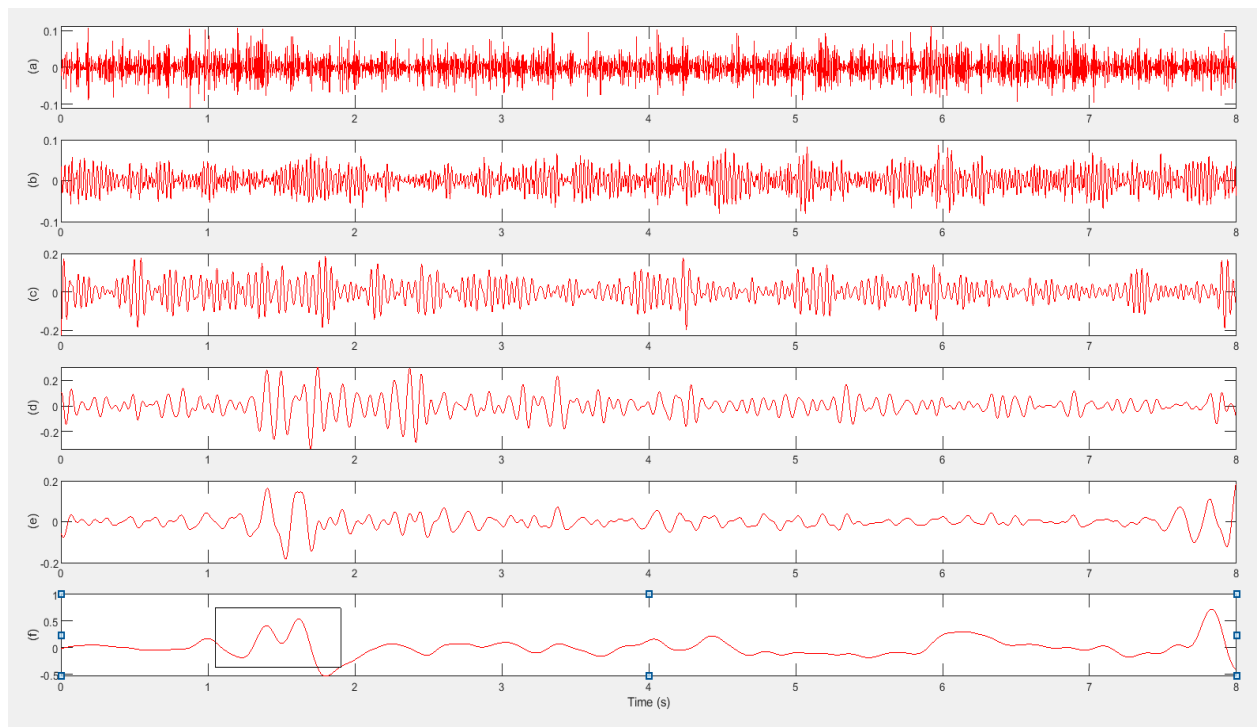


Fig5.3.1.3: Decomposed cerebral activities of EEG by SSA method.(a)67.62Hz (b) and (c) beta bands (d) 11.474 Hz (e) 5.127 Hz (f)EOG Artifact.

### 5.3.1.4 SSA-ICA

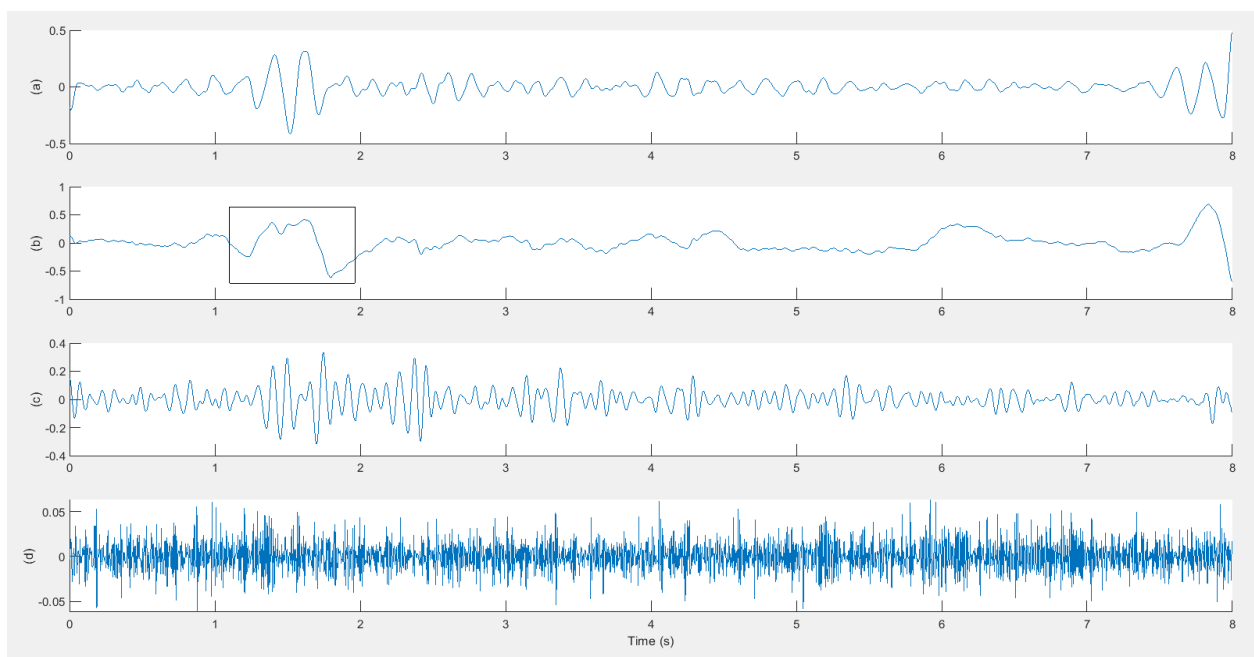


Fig5.3.1.4: Decomposed cerebral activities of EEG by SSA-ICA method(a)5.127Hz (b) EOG Artifact(c)11.474 Hz (d) 67.62 Hz.



### 5.5.1 Proposed Method

The separation of the EOG component and other cerebral activity components using proposed SSA-ICA with wavelet thresholding technique is shown in Fig. 5.3.2.1. For effective performance the length of SSA window  $L$  is assumed as 50 and the thresholding operation is performed by SWT. From Fig. 5.3.2.1, the separated EOG component is highlighted by the square shape and it can be clearly seen that the separation of the eye blink component is done quite accurately.

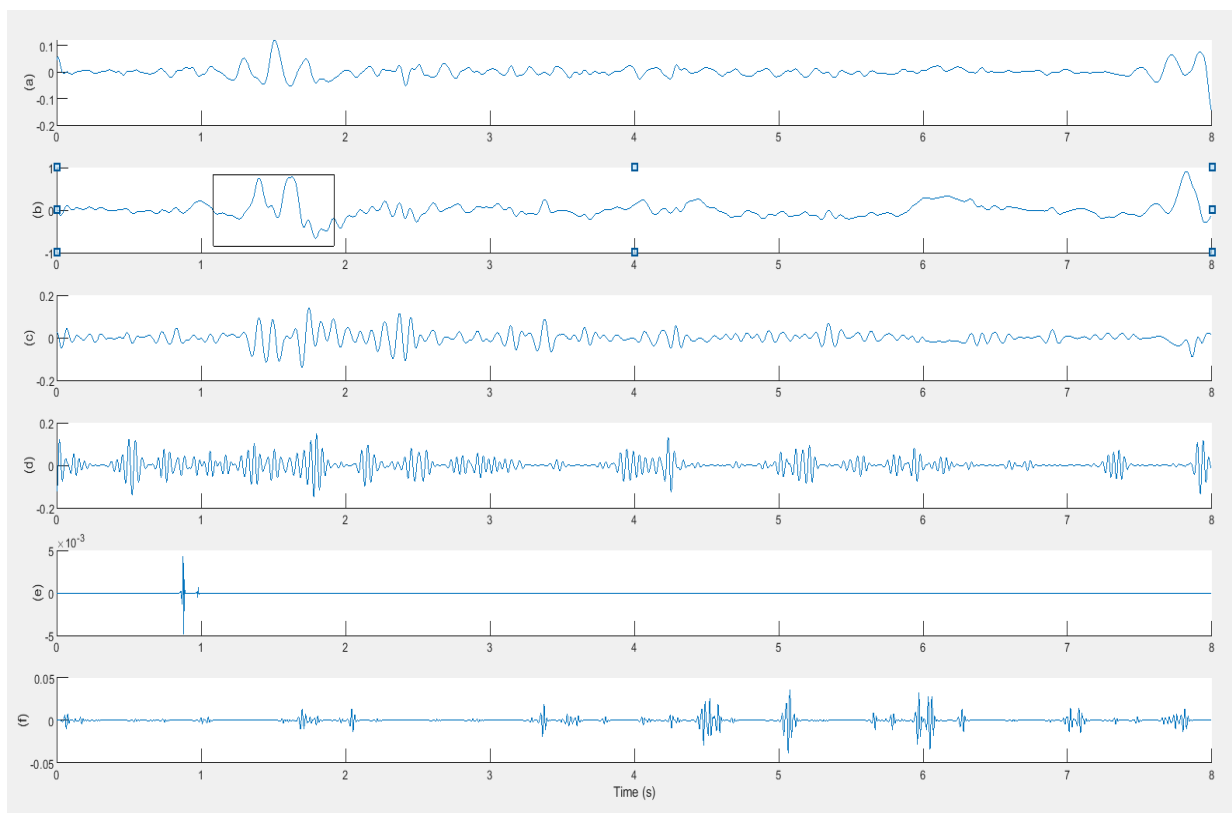


Fig 5.3.2.1: Decomposed cerebral activities of EEG by proposed SSA-ICA with wavelet thresholding method. (a) 5.127 Hz (b) EOG Artifact (c) 11.474 Hz (d) and (f) beta bands (e) Electrode pop.



---

## **CHAPTER – 6**

### **CONCLUSION AND FUTURE SCOPE**

#### **6.1 Conclusion**

The joint use of SSA-ICA with wavelet thresholding technique is presented in this work, to remove EOG artifact and to separate different activity components from single channel contaminated signal. Simulation results show that the proposed technique is more efficient to separate the sources when compared with the existing techniques such as EEMD, EEMD-ICA, SSA and SSA – ICA. The main advantage of the proposed SSA-ICA with wavelet thresholding technique is that, it retrieves the EEG component in  $\alpha$  band with high accuracy along with the separation of different cerebral activity components available in mixed EEG. Simulation results on synthetic and real EEG data demonstrate the efficiency of the proposed technique over existing methods in terms of RRMSE and MAE. Hence, it can be concluded that the SSA-ICA with wavelet thresholding method has the capability of operating on single channel EEG signals without altering the EEG  $\alpha$  component, and thus it can be applied for BCI applications.

#### **6.2 Future scope**

In our proposed algorithm it contains three stages, hence this algorithm complexity will increase. So in future number of stages will be reduced by introducing simplified algorithms.

SSA algorithm having the high computation complexity, so in future we will replace the SSA algorithm with less computational algorithms.

In second stage of SSA, SVD is there so in future we will introduce the higher order SVD which will effectively identify the artifact than the SVD.



---

## REFERENCES

- [1] Coenen A, Fine E, Zayachkivska O. "Adolf Beck: a forgotten pioneer in electroencephalography". *Journal of the History of the Neurosciences*. (2014); 23 (3): 276–286. doi:10.1080/0964704x.2013.
- [2] Gibbs FA, Davis H, Lennox WG. "The Electro-Encephalogram in Epilepsy and in Conditions of Impaired Consciousness". *Archives of Neurology and Psychiatry*. 1935;34 (6): 1133. doi:10.1001/archneurpsyc.1935.02250240002001
- [3] J.D. Bronzino. "Principles of Electroencephalography". In: J.D. Bronzino ed. *The biomedical engineering handbook*, 1995; PP. 201-212, CRC PRESS, FLORIDA.
- [4] Johal P.K., Jain N. "Artifact removal from EEG: A comparison of techniques"; *Proceedings of the 2016 International Conference on Electrical, Electronics, and Optimization Techniques*; Chennai, Indian. 3–5 March 2016.
- [5] Jebelli H., Hwang S., Lee S. "EEG-based workers' stress recognition at construction sites". *Autom. Constr.* 2018;93:315324. doi: 10.1016/j.autcon.2018.05.027.
- [6] Garrick L.W., Robert E.K., Anita M., Jeffrey F.C., Nathan A.F. "Automatic correction of ocular artifacts in the EEG: A comparison of regression-based and component-based methods". *Int. J. Psychophysiol.* 2004; 53:105–119. doi:10.1016/j.ijpsycho.2004.03.007.
- [7] Berg P, Scherg M. "Dipole models of eye movements and blinks". *Electroencephalogram Clin Neurophysiol* 1991;79:36-44.
- [8] Iwasaki M, Kellinghaus C, Alexopoulos AV, et al. "Effects of eyelid closure, blinks, and eye movements on the electroencephalogram". *Clin Neurophysiol* 2005; 116:878-885.
- [9] Hamal A.Q., Rehman A.W.B.A. "Artifact Processing of Epileptic EEG Signals: An Overview of Different Types of Artifacts"; *Proceedings of the 2013 International Conference on Advanced Computer Science Applications and Technologies*; Kuching, Malaysia. 22–24 December 2013.



- [10] Goncharova I.I., Mcfarland D.J., Vaughan T.M., Wolpaw J.R. “EMG contamination of EEG: Spectral and topographical characteristics”. *Clin. Neurophysiol* 2003; 114:1580–1593. doi: 10.1016/S1388-2457(03)00093-2.
- [11] Dirlich G, Vogl L, Plaschke M, Strian F. “Cardiac field effects on the EEG”. *Electroencephalogram Clin Neurophysiol* 1997; 102:307-315.
- [12] N.E. Huang, M.L. Wu, S.R. Long, “The empirical mode decomposition and the hilbert spectrum for nonlinear and non-stationary time series analysis”, *Proc.R.Soc.London* 454(1971)(1998)903993, <http://dx.doi.org/10.1098/rspa.1998.0193>.
- [13] Tatjana Zikov, Stkphane Bibian, Guy A. Durnont, Mihai Huzmezan, Craig R.Ries, “A wavelet based de-noising technique for ocular artifact correction of the electroencephalogram,” in: *Proceedings of the Second Joint EMBS/BMES Conference, Houston, TX, USA, 2002, pp. 23–26, <http://dx.doi.org/10.1109/IEMBS.2002.1134407>*.
- [14] A.R. Teixeira, A.M. Tomé, E.W. Lang, P. Gruber, A. Martins da Silva, “Automatic removal of high-amplitude artefacts from single-channel electroencephalograms”, *Comput. Methods Programs Biomed.* 83 (2) (2006) 125–138, <http://dx.doi.org/10.1016/j.cmpb.2006.06.003>.
- [15] Z. Wu, N.E. Huang, “Ensemble empirical mode decomposition: A noise-assisted data analysis method”, *Adv. Adapt. Data Anal.* 1 (1) (2009) 1–41, <http://dx.doi.org/10.1142/S1793536909000047>.
- [16] B. Chen, Z. He, X. Chen, H. Cao, G. Cai, Y. Zi, “A demodulating approach based on local mean decomposition and its application of mechanical fault diagnosis”, *Meas. Sci. Technol.* 22 (5) (2011) 557–604, <http://dx.doi.org/10.1088/0957-0233/22/5/055704>.
- [17] H. Peng, B. Hu, Q. Shi, M. Ratcliffe, Q. Zhao, Y. Qi, G. Gao, “Removal of ocular artifacts in EEG – an improved approach combining DWT and ANC for portable applications”, *IEEE J. Biomed. Health Inform.* 17 (3) (2013) 600–607, <http://dx.doi.org/10.1109/JBHI.2013.2253614>.
- [18] A.K. Maddirala, R.A. Shaik, “Removal of EOG artifacts from single channel EEG signals using combined singular spectrum analysis and adaptive



noisecanceler”, IEEE Sens. J. 16 (2016) 8279–8287, <http://dx.doi.org/10.1109/JSEN.2016.2560219>

[19] Ajay Kumar Maddirala, Rafi Ahamed Shaik, ”Separation of sources from single-channel EEG signals using independent component analysis”, IEEE Trans. Instrum. Meas. 67 (2) (2018) 382–393, <http://dx.doi.org/10.1109/TIM.2017.2775358>.

[20] M.E. Davies, C.J. James,” Source separation using single channel ICA”, Signal Process. 87 (8) (2007) 1819–1832, <http://dx.doi.org/10.1016/j.sigpro.2007.01.011>.

[21] M. Ghil et al., “Advanced spectral methods for climatic time series,” Rev.Geophys., vol.40,no.1,pp.1–41,Sep.2002.

[22] N. Golyandina, V. Nekrutkin, and A. A. Zhigljavsky, Analysis of Time Series Structure: SSA and Related Techniques (Monographs on statistics and applied probability), vol. 90. Boca Raton, FL, USA:Chapman & Hall, 2001.

[23] M. Meraha, T.A. Abdelmalika, B.H. Larbic, R-peaks detection based on stationary wavelet transform, Comput. Methods Programs Biomed. 121 (3) (2015) 149–160, <http://dx.doi.org/10.1016/j.cmpb.2015.06.003>.

[24] J.C. Pesquet, H. Krim, H. Carfatan, Time-invariant orthonormal wavelet representations, IEEE Trans. Sig.Process. 44 (1996) 1964–1970.

[25] S. Mallat, A Wavelet Tour of Signal Processing, Acad. Press, San Diego, CA, 1999.

[26] Tatjana Zikov, Stkphane Bibian, Guy A. Durnont, Mihai Huzmezan, Craig R. Ries, A wavelet based de-noising technique for ocular artifact correction of the electroencephalogram, in: Proceedings of the Second Joint EMBS/BMES Conference, Houston, TX, USA, 2002, pp. 23–26, <http://dx.doi.org/10.1109/IEMBS.2002.1134407>.

[27] David L. Donoho, De-noising by soft-thresholding, IEEE Trans. Inf. Theory 41 (3)(1995) 613–627, <http://dx.doi.org/10.1109/18.382009>.

[28] M. Tangermann, K.-R. Miller, A. Aertsen, N. Birbaumer, C. Braun, C. Brunner, R. Leeb, C. Mehring, K.J. Miller, G. Mueller-Putz, G. Nolte, G. Pfurtscheller, H. Preissl, G. Schalk, A. Schlgl, C. Vidaurre, S. Waldert, B.



---

Blankertz, Review of theBCI competition IV, *Front. Neurosci.* 6 (55) (2012)  
<http://dx.doi.org/10.3389/fnins.2012.00055>.

[29] A. Schlogl, C. Keinrath, D. Zimmermann, R. Scherer, R. Leeb, G. Pfurtscheller, A fully automated correction method of EOG artifacts in EEG recordings, *Clin. Neurophysiol.* 118 (1) (2007) 98–104,  
<http://dx.doi.org/10.1016/j.clinph.2006.09.003>.